Available online at www.sciencedirect.com
ScienceDirect
Journal of Environmental Sciences 2011, 23(11) 1911–1918
JOURNAL OF ENVIRONMENTAL SCIENCES
ISSN 1001-0742
CN 11-2629/X
www.jesc.ac.cn

Photocatalytic degradation kinetics and mechanism of pentachlorophenol based on superoxide radicals

Yang Li, Junfeng Niu*, Lifeng Yin, Wenlong Wang, Yueping Bao, Jing Chen, Yanpei Duan

State Key Laboratory of Water Environment Simulation, School of Environment, Beijing Normal University, Beijing 100875, China. E-mail: liyang_bnu@yahoo.cn

Received 09 November 2010; revised 06 December 2010; accepted 10 December 2010

Abstract

The micron grade multi-metal oxide bismuth silicate ($Bi_{12}SiO_{20}$, BSO) was prepared by the chemical solution decomposition technique. Photocatalytic degradation of pentachlorophenol (PCP) was investigated in the presence of BSO under xenon lamp irradiation. The reaction kinetics followed pseudo first-order and the degradation ratio achieved 99.1% after 120 min at an initial PCP concentration of 2.0 mg/L. The pH decreased from 6.2 to 4.6 and the dechlorination ratio was 68.4% after 120 min at an initial PCP concentration of 8.0 mg/L. The results of electron spin resonance showed that superoxide radical ($O_2^{\cdot -}$) was largely responsible for the photocatalytic degradation of PCP. Interestingly, this result was different from that of previous photocatalytic reactions where valence band holes or hydroxyl radicals played the role of major oxidants. Some aromatic compounds and aliphatic carboxylic acids were determined by GC/MS as the reaction intermediates, which indicated that $O_2^{\cdot -}$ can attack the bond between the carbon and chlorine atoms to form less chlorinated aromatic compounds. The aromatic compounds were further oxidized by $O_2^{\cdot -}$ to generate aliphatic carboxylic acids which can be finally mineralized to CO_2 and H_2O.

Key words: photocatalytic degradation; pentachlorophenol; bismuth silicate; superoxide radicals; reaction mechanisms

DOI: 10.1016/S1001-0742(10)60563-3

Citation: Li Y, Niu J F, Yin L F, Wang W L, Bao Y P, Chen J et al., 2011. Photocatalytic degradation kinetics and mechanism of pentachlorophenol based on superoxide radicals. Journal of Environmental Sciences, 23(11): 1911–1918

Introduction

Pentachlorophenol (PCP) has been extensively used as wood preservative, herbicide or biocide throughout the world (Orton et al., 2009). Because of its high toxicity and chemical stability, it has been listed as priority pollutants by US EPA (Meunier, 2002). What is more, it can be transformed into more toxic polychlorinated dibenzo-*p*-dioxins (PCDDs) and polychlorinated dibenzofurans (PCDFs) (Ho et al., 2010). Therefore, it is of great importance to develop environmentally friendly techniques to eliminate PCP in the environment.

Photocatalytic degradation has received considerable attention because of its efficiency in the elimination of low concentrations of recalcitrant organic pollutants from the aqueous solution (Zhang et al., 2009; González et al., 2010). It has been well established that this technology mainly works on the generation of various reactive active species such as hydroxyl radicals (·OH), superoxide radicals ($O_2^{\cdot -}$), and valence band holes (h_{vb}^+) which can undergo redox reactions with most persistent organic compounds and convert them into less harmful compounds or completely mineralize them into CO_2 and H_2O (Tang et al., 2004; Ji and Chu, 2009; Jiang et al., 2009; Rao and Chu, 2009; Yang et al., 2009a).

The majority of publications reported ·OH as the major oxidants for the photocatalytic degradation (Gao et al., 2007; Yang et al., 2009b; Fukushima and Tatsumi, 2001). In these reactions, ·OH can react with organic substances by hydroxylation through ·OH addition onto the organic molecule, followed by further oxidation. However, there was much debate with respect to the reactive active species which played a decisive role during photocatalytic degradation. For example, by examining TiO_2 photocatalytic oxidation of arsenite system, Yoon and Lee (2005) concluded that h_{vb}^+ was the major oxidant; Lee and Choi (2002) proposed $O_2^{\cdot -}$ as the dominant oxidant; while Dutta et al. (2005) suggested ·OH as the major reactive active species. Several studies demonstrated that $O_2^{\cdot -}$ could be the major oxidant in photocatalytic reactions (Song et al., 2007). However, no further information about the detailed reaction mechanisms based on $O_2^{\cdot -}$ was provided.

Bismuth silicate crystal is a conventional photorefractive, electro-optic material with good photoconductivity. In 2006, He and Gu (2006) firstly studied the photocatalytic

* Corresponding author. E-mail: junfengn@bnu.edu.cn

activity of BSO. They found that the intrinsic oxygen defects in BSO can act as photogenerated electron traps and thus suppress the recombination of electron-hole pairs. While notable photocatalytic activity was achieved, two challenges remained: (1) to investigate the main active radicals of the catalyst that induces the photocatalytic degradation of organic compounds, and (2) to improve the recovery rate of the catalyst when it is used for wastewater treatment.

In this work, we prepared bismuth silicate ($Bi_{12}SiO_{20}$, BSO) by the chemical solution decomposition (CSD) technique and further investigated its photocatalytic activity for pentachlorophenol (PCP) under simulated sunlight irradiation. The active species during the photocatalytic degradation of PCP were examined and the possible photocatalytic degradation pathway was proposed.

1 Experimental section

1.1 Preparation of the catalyst

The precursor materials of BSO crystal was prepared by the CSD technique. The compounds, $Bi(NO_3)_3{\cdot}5H_2O$ and $Si(OC_2H_5)_4$, were selected as the bismuth and silicon source, respectively. Glacial acetic acid (HAC; 99.7%) was used as a solvent. Poly(alkylene oxide) block copolymers, $HO(CH_2CH_2O)_{122}$-$(CH_2CH$-$(CH_3)O)_{56}$-$(CH_2CH_2O)_{122}H$ (Pluronic F-108; BASF), were used as pore-forming agents. Firstly, $Bi(NO_3)_3{\cdot}5H_2O$ was dissolved in CH_3COOH, then $Si(OC_2H_5)_4$ was added dropwise to the above solution with constant stirring. The solution was aged with stirring for 12 hr at 30°C . Prior to calcination, the resultant solution was added to stainless steel autoclaves with a teflon liner. After being sealed, the autoclaves were heated in a convection oven at 150°C for 24 hr and allowed to cool to room temperature afterwards. The resulting products were filtered off, washed with deionized water several times and then dried at 120°C for 4 hr to remove the solvent. The obtained precursor powders were calcinated at 550°C for 3 hr in air, and then ground into fine powders in an agate mortar.

1.2 Characterization of BSO

X-ray diffraction (XRD) analysis was recorded using a diffractometer with Cu$K\alpha$ radiation (X' Pert PRO MPD; PW3040/60, Holland). The accelerating voltage and the scan rate were 40 kV and 2 min^{-1}, respectively.

Diffuse reflectance absorption spectra (DRS) of the catalyst was recorded on a UV-Visible spectrophotometer (Specord 200; Analytik Jena, Germany) equipped with an integrated sphere attachment.

Electron spin resonance spectrometry (ESR; Bruker ESP-300E, Germany) was employed to determine the photosensitized reactive oxygen species (ROS). The setting of the ESR spectrometer was as follows: center field 3480.00 G; microwave power 10 mW; receiver gain 1.00×10^5; modulation frequency 100.00 kHz; modulation amplitude 2.071 G; conversion 40.96 msec; sweep width 100.00 G; sweep time 41.943 sec.

1.3 Photocatalytic degradation of PCP

The photocatalytic activity of BSO for the degradation of PCP in the aqueous solution was tested under a xenon lamp (CHF-XM-500W; Trusttech, China) in the range of 300–800 nm. A weight of 50 mg powder was dispersed in a 200-mL solution containing PCP at an appropriate concentration (2.0, 4.0, 6.0, 8.0, or 10.0 mg/L). Prior to irradiation, the suspension of catalyst in the PCP solution was firstly ultrasonicated for 15 min and then stirred for 30 min in dark to achieve an adsorption-desorption equilibrium. After 15 min, the ultrasonication exhibited so minor effect on PCP removal ratio that it cannot be detected. Suspension was then irradiated under the above light source with constant stirring. The reaction temperature was kept at (20 ± 2)°C by a constant-temperature water bath. The distance between the liquid surface and the light source was about 20 cm.

The stability of the catalysts was investigated by the circular photodegradation experiments that were carried out under the same reaction conditions as above mentioned. After evaluating the photocatalytic activity of BSO for the first time, the aqueous solution was centrifuged to recycle the BSO powders that were then washed with ethanol and dried at room temperature before reuse. The recycling period was set to 2 hr.

1.4 Analytical determination and product identification

High-performance liquid chromatography (HPLC; Waters, USA) was used to analyze the concentration of PCP. First, a volume of 20 μL sample was injected into the HPLC running on the mobile phase of 85:15 (V/V) of methanol/ammonium acetate. The separation was performed using an ODS-18 reversed phase column (5 μm, 150 mm × 4.6 mm) at the flow rate of 1 mL/min and column temperature of (20 ± 2)°C. A UV detector was set at 312 nm. All samples were immediately analyzed to avoid further reaction.

The concentration of Cl^- was analyzed using an ion chromatography (DX-600; Dionex, USA). The pH value was measured by pH meter (PB-10; Sartorius, Germany).

Degradation intermediates were analyzed using gas chromatograph-mass spectrometer (GC/MS; Varian, USA). GC/MS analysis was performed on a GC (3900N)/MS (4000) system equipped with a DB-5 column (J&W, USA). The injector temperature was set at 280°C. Helium served as the carrier gas at a constant flow of 1.0 mL/min (He, 99.999%). The column temperature was kept at 80°C for 6 min, linearly raised at 4°C/min to 180°C afterwards, and then remained at 180°C for 10 min. Five libraries (MAINLIB, REPLIB, TUTORIAL, MS and LL) were used to identify the intermediates and the results were further confirmed by injection of standard solutions.

2 Results and discussion

2.1 Characterization of BSO

The XRD pattern of the prepared catalyst is presented in Fig. 1. The sharp and well defined signals were in good

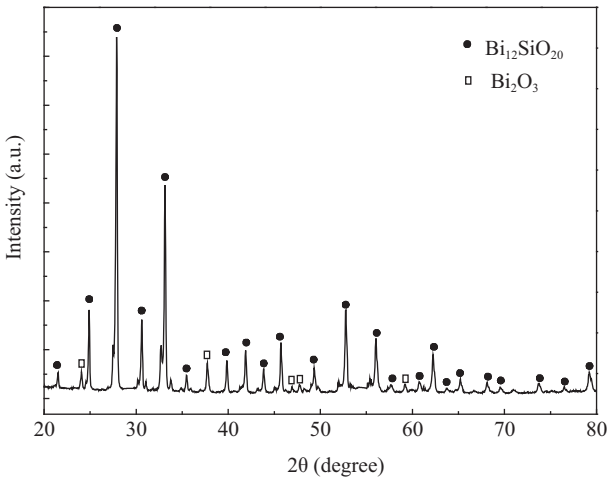

Fig. 1 XRD pattern of the prepared catalyst calcined at 550°C for 3 hr.

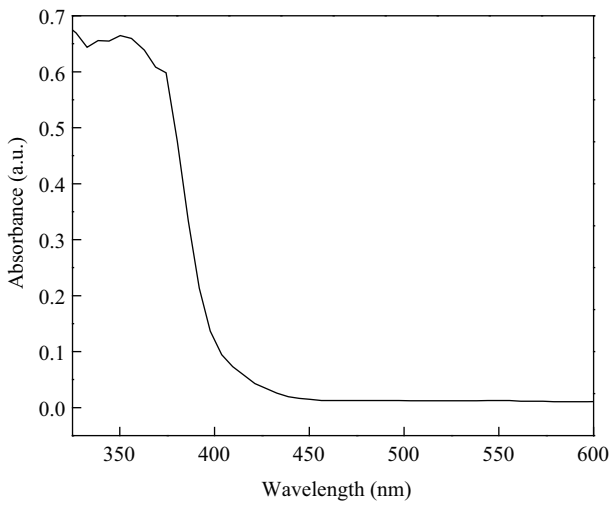

Fig. 2 UV-Visible diffuse reflectance absorption spectra of BSO calcined at 550°C for 3 hr.

agreement with the already known profile of crystalline cubic silicate (BSO) (Inorganic Crystal Structure Database (ICSD), National Institute of Standards and Technology Ref. No. 01-080-0627), except for several weak signals matching with the anorthic oxide (Bi_2O_3) (ICSD, National Institute of Standards and Technology Ref. No. 00-050-1088). The low intensity and small amounts of such signals suggested that part of the Bi element was incorporated into the dominant structure but the amount of the anorthic phase was negligible. The single sharp peak with high intensity at around 28° showed a high degree of crystallinity of the prepared catalyst (He and Gu, 2006).

The average crystal size (D) of BSO was calculated according to the Debye-Scherrer equation as the following (Yao et al., 2004):

$$D = \frac{0.89\lambda}{B\cos\theta}$$

where, λ is the incident wavelength of X-ray light, B and θ are peak half-width and semi-angle of diffraction corresponding to the most intensive diffraction peak, respectively. The size calculated was about 400 nm.

The BET specific surface area of BSO was 3.6 m^2/g, whereas $BiFeO_3$ was 1.2 m^2/g (Gao et al., 2007) and $CaBi_2O_4$ was 0.6 m^2/g (Tang et al., 2004). The results indicated that BSO molecules could load more organic contaminants because of its high surface area, facilitating PCP molecules access to the reactive sites on the surface of BSO and thus enhancing the degradation efficiency of PCP (Iskanda et al., 2007).

DRS analysis was used to evaluate the photoabsorption capacity of photocatalyst. Figure 2 illustrates the UV-Visible diffuse reflectance spectroscopy of BSO. The results indicated that the BSO powder could absorb visible light in the range of 400–550 nm, which was in agreement with the yellow colour of the synthesized samples.

2.2 Photocatalytic degradation of PCP in the presence of BSO

Photocatalytic degradation results of PCP at different initial concentrations are presented in Fig. 3. After 120 min, the photocatalytic degradation ratios of PCP at initial

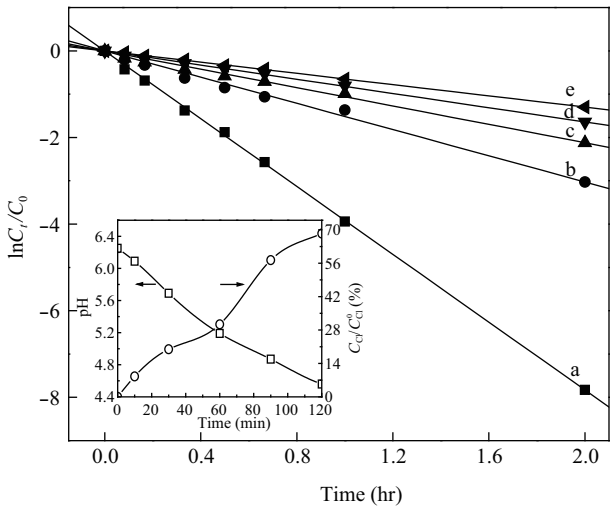

Fig. 3 Photocatalytic degradation kinetics of PCP in BSO suspension at different initial concentrations. Line a: 2.0 mg/L; line b: 4.0 mg/L; line c: 6.0 mg/L; line d: 8.0 mg/L; line e: 10.0 mg/L. Inset: change of pH and evolution of the Cl^- ion during the photocatalytic degradation of PCP at an initial concentration of 8.0 mg/L. The reactions were done at pH = 6.1, BSO loading 250.0 mg/L.

concentrations of 2.0, 4.0, 6.0, 8.0, and 10.0 mg/L were 99.1%, 95.2%, 88.0%, 80.6%, and 72.7%, respectively. The lower the initial concentration of PCP was, the higher the degradation efficiency was. We also proved that at the same initial PCP concentration of 10.0 mg/L, increasing the catalyst loading from 250.0 to 500.0 mg/L could increase the degradation ratio of PCP. These phenomena were explained by the fact that at the same catalyst loading the number of the generated active radical species was identical. At lower initial concentrations, PCP molecules were more liable to the attack of reactive species due to the higher ratio of reactive species to PCP, resulting in higher degradation efficiency.

The linear correlation between $\ln C_t/C_0$ and time suggested that the photocatalytic degradation of PCP followed pseudo first-order kinetics. Meanwhile, the photolysis of PCP at initial concentration of 10.0 mg/L was unapparent and the concentration decreased to 9.3 mg/L in 120 min. After 120 min, the PCP removal ratio of BSO under dark

condition at initial concentration of 10.0 mg/L was 7.1%, indicating that BSO could hardly initiate PCP degradation without light irradiation.

Variations of pH and formation of chloride ions in the reaction solution are displayed in the inset in Fig. 3. The pH values of the solution decreased from 6.2 to 4.6 in 120 min, which was probably attributed to the generation of aliphatic carboxylic acids. After 120 min, about 68.4% of the organic chlorine was released into the reaction solution in the form of inorganic ions, suggesting that the degradation of PCP was accompanied with a dechlorination process. Similar phenomena were also reported by Gunlazuardi and Lindu (2005), who found that the photocatalytic degradation of PCP led to a complete dechlorination over TiO_2 film.

Conclusively, BSO exhibited high photocatalytic activity to remove PCP from aqueous solution. These phenomena were explained by the fact that the intrinsic oxygen vacancies in the crystal lattice of BSO could favor the interfacial electron transfer, preventing the recombination of electron–hole pairs (Wang et al., 2008). Moreover, the valence band of the multi-metal oxides mainly originated from the hybridization of the O 2p and Bi 6s orbits. The hybrid orbit formed a widely dispersed valence band, which was beneficial to the mobility of the holes and increased the probability of holes reaching the reaction sites on the surface of the catalyst. In the present study, the XRD results showed that BSO photocatalyst had a high degree of crystallinity which could create more possible reactive sites on the surface of BSO.

2.3 Active species to attack PCP

ESR spin trap technique was conducted to investigate the reactive radicals generated by BSO. The compound, 5,5-dimethyl-1-pyrroline-*N*-oxide (DMPO) was used as the spin trapping chemical (Yu et al., 2005; Hu et al., 2006). As shown in Fig. 4, six characteristic peaks of the DMPO-$O_2^{\cdot-}$ spin adducts could be found under light irradiation while no such signal was detected without direct light irradiation (Fig. 4a, b). Moreover, no DMPO-·OH signal was detected with or without light irradiation (Fig. 4c, d). These results suggested that $O_2^{\cdot-}$ was produced on the catalyst surface and may govern the photocatalytic oxidation of PCP.

To ascertain the presence of $O_2^{\cdot-}$, comparison experiments of N_2-purged condition and scavenger-loaded condition were undertaken. Three radical scavengers were utilized during the photocatalytic degradation of PCP, including azide (NaN_3), 1,4-benzoquinone ($C_6H_4O_2$) and potassium iodide (KI). NaN_3 is an $^1O_2$ quencher but may also interact with ·OH (Xu et al., 2008), $C_6H_4O_2$ selectively quenches $O_2^{\cdot-}$ (Zhang et al., 2009) and KI reacts with both positive holes (h_{vb}^+) and ·OH on catalyst surface (Yang et al., 2009a).

As shown in Fig. 5, the notable result was that the photocatalytic degradation ratio in the air equilibrium condition was 87.0%, clearly higher than that in the N_2 condition which was only about 17.4%. Under the N_2-purged conditions, dissolved or adsorbed O_2 might be sufficient to degrade PCP at the early stage but the degradation stopped after O_2 was used up, indicating O_2

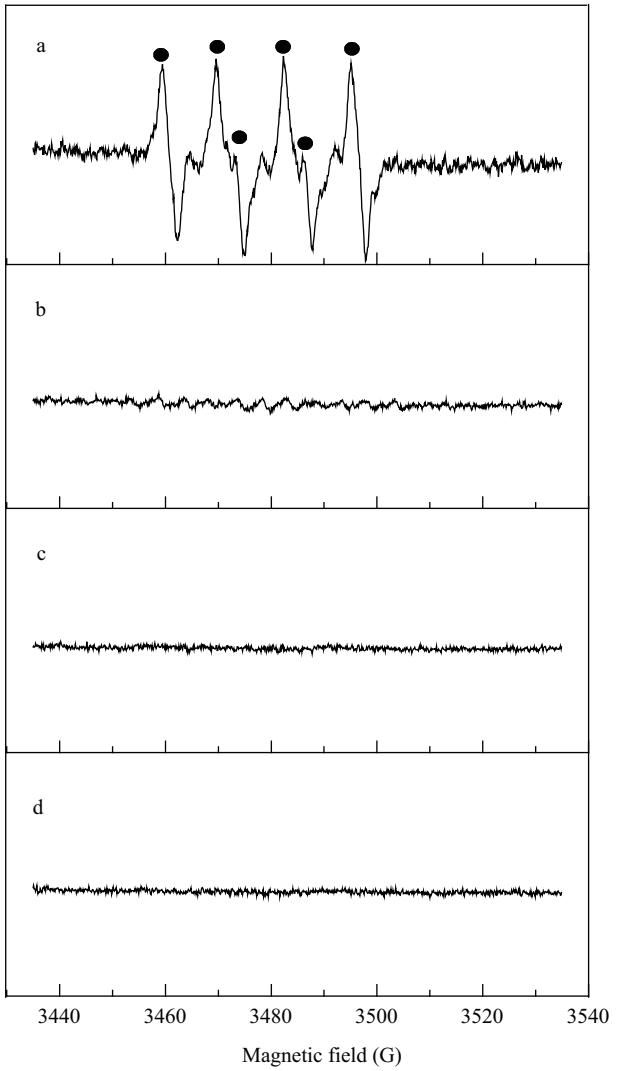

Fig. 4 ESR spectra recorded at ambient temperature for DMPO-$O_2^{\cdot-}$ under irradiation of 355 nm (a), DMPO-$O_2^{\cdot-}$ without direct irradiation (b), DMPO-·OH under irradiation of 355 nm (c), and DMPO-·OH without direct irradiation (d).

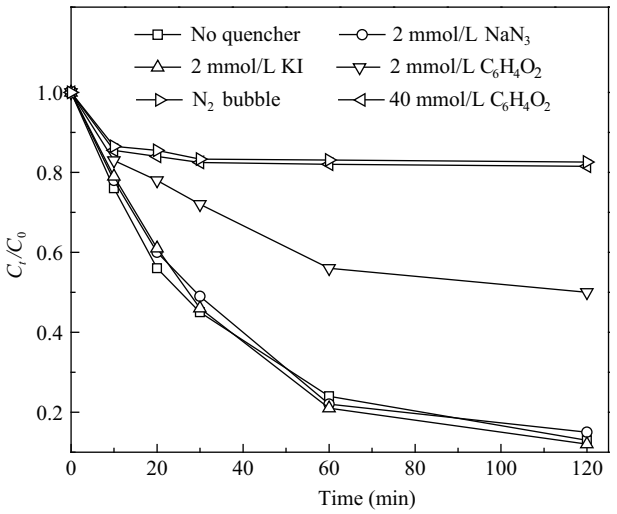

Fig. 5 Effect of radical scavenger on photocatalytic degradation of PCP at pH = 6.1, BSO loading 250.0 mg/L and initial PCP concentration 4.0 mg/L.

was the main source of the active species.

The effects of radical scavengers on PCP photocatalytic degradation are shown in Fig. 5. It was observed that the addition of 2 mmol/L NaN_3 and KI caused slight change in the photocatalytic degradation rate of PCP, indicating that h^+_{vb}, $^1O_2$ and ·OH were not the main active species involved in the photocatalytic degradation process. At least, the concentrations of h^+_{vb}, $^1O_2$ and ·OH were too low to oxidize PCP. However, a concentration of 2 mmol/L $C_6H_4O_2$ caused reduction in the PCP removal, which decreased from 87.0% to 50.6% after 120 min. Furthermore, a strong suppressing effect on PCP degradation was observed after the addition of 40 mmol/L of $C_6H_4O_2$. The removal ratio decreased from 87.0% to 18.5% after 120 min using the quencher, indicating that $O_2^{\cdot -}$ played a predominant role in PCP photocatalytic degradation, which was in agreement with the ESR results. Furthermore, our previous research also detected $O_2^{\cdot -}$ during the photocatalytic degradation of PCP by Ti-doped Bi_2O_3 under visible light irradiation (Yin et al., 2010a).

It can be concluded from this present study that BSO can absorb the photons at energies greater than the band gap energies to generate electron-hole pairs. The photogenerated electrons of BSO conduction band were scavenged by the dissolved or adsorbed O_2 on the surface of BSO to produce $O_2^{\cdot -}$, which could further form hydrogen peroxide (H_2O_2), hydroperoxy radical ($HO_2^{\cdot}$) and ·OH (Jiang et al., 2009). The active species could initiate a series of redox reactions to mineralize adsorbed PCP molecules into CO_2 and H_2O (Huang et al., 2008).

2.4 Determination of PCP photocatalytic degradation intermediates

To further understand the photocatalytic degradation mechanisms of PCP, GC/MS was applied to identify the intermediates. The formation and decay of several intermediates are provided in Fig. 6. In the present study, thirteen photocatalytic intermediates of PCP were indentified. After 10 min, five kinds of aromatic intermediates were detected by GC/MS, including tetrachlorophenols (TeCP), trichlorophenols (TCP), dichlorophenols (DCP), chlorophenols (CP), and phenol. The concentration of these aromatic intermediates increased initially and then decreased gradually and almost disappeared after irradiation for 180 min. Aliphatic carboxylic acids (such as malonic acid) increased in concentration throughout the reaction (up to 180 min), implying the continual mineralization of aromatic intermediates.

On the basis of these intermediates and the corresponding concentration change, the photocatalytic degradation pathway for PCP was proposed (Fig. 7). Because chlorine was an electron-withdrawn group, the carbon atoms of the benzene ring were electropositive and were able to attract electrons (Weavers et al., 2000; Luo et al.,

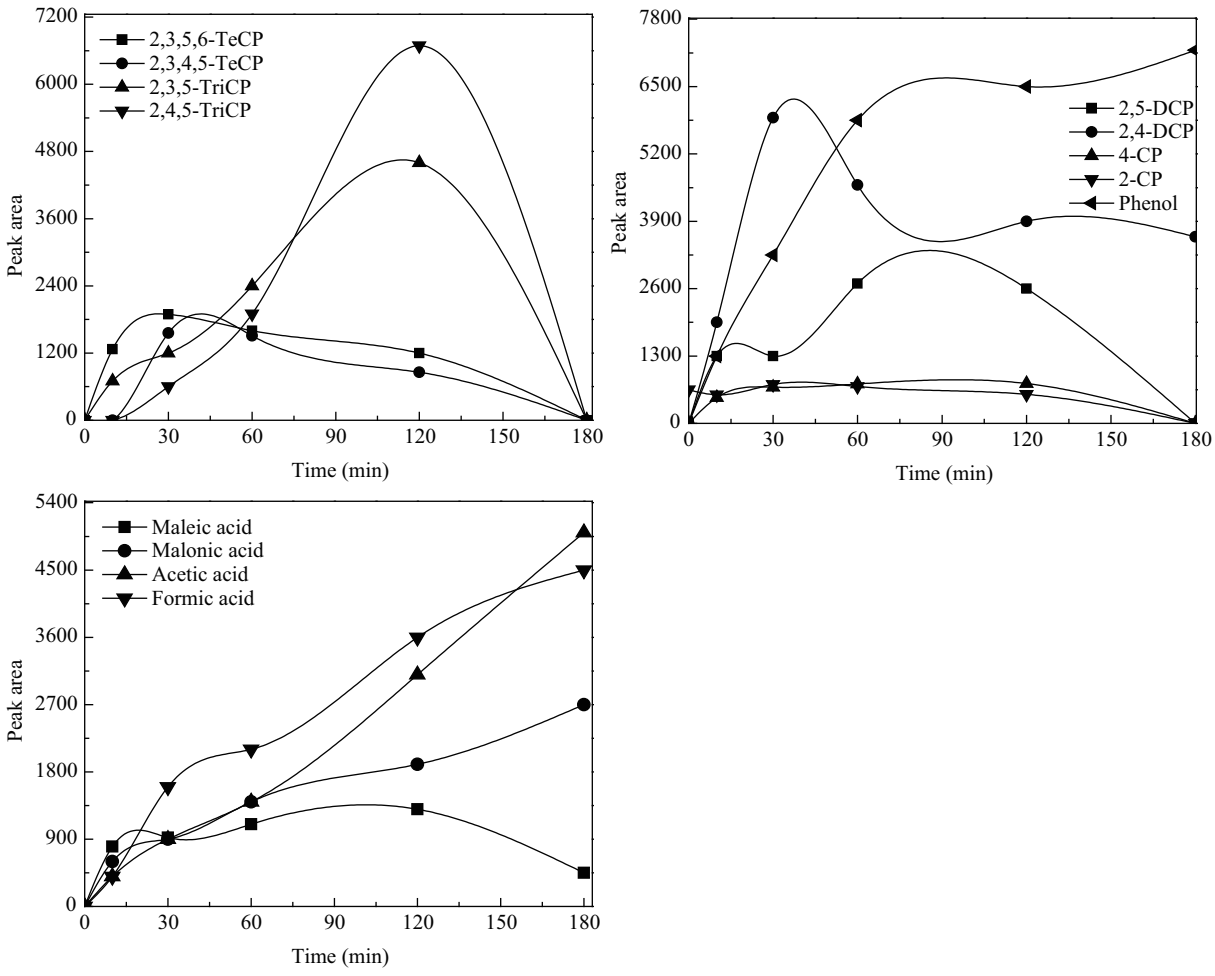

Fig. 6 Identified intermediates and variations of their peak area during photocatalytic degradation of PCP.

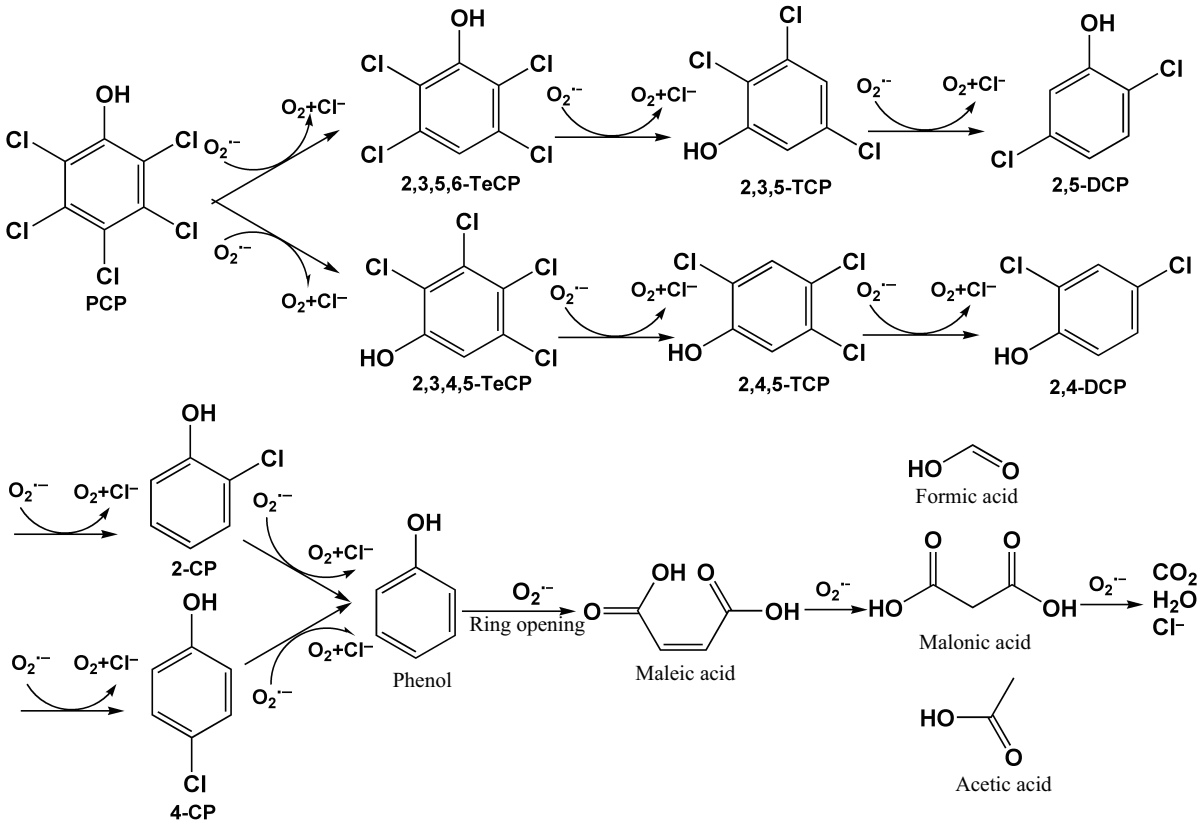

Fig. 7 Possible reaction pathways during photocatalytic degradation of PCP.

2008). Meanwhile, plenty of $O_2^{\cdot-}$ radicals generated in the solution were strongly nucleophilic to release electrons. They could attack the carbon atoms to cleave the bond between the carbon and chlorine atoms. Therefore, the chlorine atoms in the PCP molecule could be gradually cleaved to form a series of less chlorinated congeners and phenol. In our previous experiments, TeCP was also reported as the main intermediates of PCP photocatalytic degradation (Yin et al., 2010b). Furthermore, $O_2^{\cdot-}$ is a moderate oxidant with reduction potential ($E^0(O_2^{\cdot-})/HO_2^{\cdot}$) = 1.7 V; $E^0(O_2^{\cdot-})/H_2O_2$) = 1.7 V), which suffices to oxidize organic compounds (Song et al., 2007). Phenol was oxidized to form maleic acid. All these aromatic intermediates generated would undergo further oxidation to form aliphatic carboxylic acids (such as malonic acid). As a result, a pH decrease was consistently observed during our experiments. Similar results were also reported by Lan et al. (2008). As the photocatalytic degradation proceeded, the small aliphatic carboxylic acids could be mineralized into carbon dioxide and water. This pathway was consistent with previous report of PCP photocatalytic degradation under UV light irradiation (Suegara et al., 2005). Although quinones were reported as main photocatalytic degradation intermediates of PCP (Sivalingam et al., 2004), they were not detected in the present study.

2.5 Stability of the photocatalyst

The stability of a photocatalyst is important for its practical application. During repeated degradation processes, degeneration of catalytic activity may occur. Therefore, a series of photocatalytic experiments with recycled BSO were carried out to investigate the stability of BSO. The corresponding results are given in Fig. 8. After four times, BSO did not exhibit obvious loss of activity compared with that of the first time. The good photocatalytic stability proved that BSO was stable for the photocatalytic degradation of PCP.

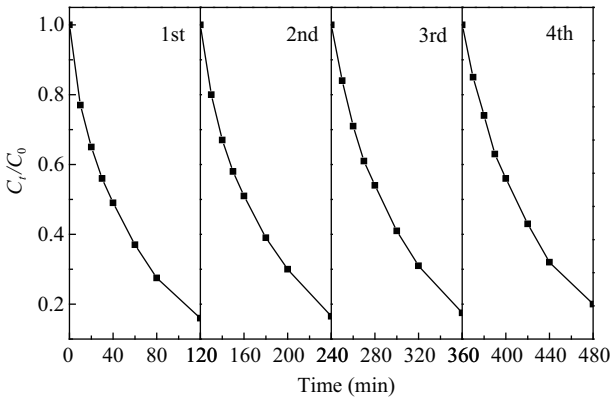

Fig. 8 PCP photocatalytic degradation with recycled BSO at pH = 6.1, photocatalyst loading 250.0 mg/L and initial concentration 4.0 mg/L.

3 Conclusions

PCP could be effectively degraded by BSO photocatalyst in aqueous solution under xenon light irradiation. The reaction followed pseudo first-order kinetics. The radical scavenger and ESR technologies showed that $O_2^{\cdot-}$ mainly led to the photocatalytic degradation of PCP. The results indicated that the photocatalytic degradation mechanisms of PCP based on $O_2^{\cdot-}$ were dechlorination and oxidation.

After four times, BSO still exhibited good photocatalytic activity compared with that of the first time.

Acknowledgments

This work was supported by the National Natural Science Foundation of China (No. 21077010), the National Key Technology R&D Program of China (No. 2008BAC32B06-3), the National High Technology Research and Development Program (863) of China (No. 2009AA05Z306) and the Program for Changjiang Scholars and Innovative Research Team in University (No. IRT0809).

References

Dutta P K, Pehkonen S O, Sharma V K, Ray A K, 2005. Photocatalytic oxidation of arsenic(III): Evidence of hydroxyl radicals. *Environmental Science and Technology*, 39(6): 1827–1834.

Fukushima M, Tatsumi K, 2001. Degradation pathways of pentachlorophenol by photo-fenton systems in the presence of iron(III), humic acid, and hydrogen peroxide. *Environmental Science and Technology*, 35(9): 1771–1778.

Gao F, Chen X Y, Yin K B, Dong S, Ren Z F, Yuan F et al., 2007. Visible-light photocatalytic properties of weak magnetic $BiFeO_3$ nanoparticles. *Advanced Materials*, 19(19): 2889–2892.

González L F, Sarria V, Sánchez O F, 2010. Degradation of chlorophenols by sequential biological-advanced oxidative process using Trametes pubescens and TiO_2/UV. *Bioresource Technology*, 101(10): 3493–3499.

Gunlazuardi J, Lindu W A, 2005. Photocatalytic degradation of pentachlorophenol in aqueous solution employing immobilized TiO_2 supported on titanium metal. *Journal of Photochemistry and Photobiology A: Chemistry*, 173(1): 51–55.

He C H, Gu M Y, 2006. Preparation, characterization and photocatalytic properties of $Bi_{12}SiO_{20}$ powders. *Scripta Materialia*, 55(5): 481–484.

Ho D P, Senthilnanthan M, Mohammad J A, Vigneswaran S, Ngo H H, Mahinthakumar G et al., 2010. The application of photocatalytic oxidation in removing pentachlorophenol from contaminated Water. *Journal of Advanced Oxidation Technologies*, 13(1): 21–26.

Hu C, Hu X X, Guo J, Qu J H, 2006. Efficient destruction of pathogenic bacteria with $NiO/SrBi_2O_4$ under visible light irradiation. *Environmental Science and Technology,* 40(17): 5508–5513.

Huang G L, Zhang S C, Xu T G, Zhu Y F, 2008. Fluorination of $ZnWO_4$ photocatalyst and influence on the degradation mechanism for 4-chlorophenol. *Environmental Science and Technology*, 42(22): 8516–8521.

Iskandar F, Nandiyanto A B D, Yun K M, Hogan C J Jr, Okuyama K, Biswas P, 2007. Enhanced photocatalytic performance of brookite TiO_2 macroporous particles prepared by spray drying with colloidal templating. *Advanced Materials*, 19(10): 1408–1412.

Ji P F, Zhang J L, Chen F, Anpo M, 2009. Study of adsorption and degradation of Acid Orange 7 on the surface of CeO_2 under visible light irradiation. *Applied Catalysis B: Environmental*, 85(3-4): 148–154.

Jiang D, Xu Y, Wu D, Sun Y H, 2009. Isocyanate-modified TiO_2 visible-light-activated photocatalyst. *Applied Catalysis B: Environmental*, 88(1-2): 165–172.

Lan Q, Li F B, Liu C S, Li X Z, 2008. Heterogeneous photodegradation of pentachlorophenol with maghemite and oxalate under UV illumination. *Journal of Hazardous Materials*, 42(21): 7918–7923.

Lee H, Choi W, 2002. Photocatalytic oxidation of arsenite in TiO_2 suspension: Kinetics and mechanisms. *Environmental Science and Technology*, 36(17): 3872–3878.

Luo T, Ai Z H, Zhang L Z, 2008. $Fe@Fe_2O_3$ core-shell nanowires as iron reagent. 4. sono-fenton degradation of pentachlorophenol and the mechanism analysis. *Journal of Physical Chemistry C*, 112(23): 8675–8681.

Meunier B, 2002. Catalytic degradation of chlorinated phenols. *Science*, 296(5566): 270–271.

Orton F, Lutz I, Kloas W, Routledge E J, 2009. Endocrine disrupting effects of herbicides and pentachlorophenol: in vitro and in vivo evidence. *Environmental Science and Technology*, 43(6): 2144–2150.

Rao Y F, Chu W, 2009. Reaction mechanism of linuron degradation in TiO_2 suspension under visible light irradiation with the assistance of H_2O_2. *Environmental Science and Technology*, 43(16): 6183–6189.

Sivalingam G, Priya M H, Madras G, 2004. Kinetics of the photodegradation of substituted phenols by solution combustion synthesized TiO_2. *Applied Catalysis B: Environmental*, 51(1): 67–76.

Song S, Xu L J, He Z Q, Chen J M, Xiao X Z, Yan B, 2007. Mechanism of the photocatalytic degradation of C.I. Reactive Black 5 at pH 12.0 using $SrTiO_3/CeO_2$ as the catalyst. *Environmental Science and Technology*, 41(16): 5846–5853.

Suegara J, Lee B D, Espino M P, Nakai S, Hosomi M, 2005. Photodegradation of pentachlorophenol and its degradation pathways predicted using density functional theory. *Chemosphere*, 61(3): 341–346.

Tang J W, Zou Z G, Ye J H, 2004. Efficient photocatalytic decomposition of organic contaminants over $CaBi_2O_4$ under visible-light irradiation. *Angewandte Chemie International Edition*, 43(34) : 4463–4466.

Wang Y, Wang Y, Meng Y L, Ding H M, Shan Y K, Zhao X et al., 2008. A highly efficient visible-light-activated photocatalyst based on bismuth- and sulfur-codoped TiO_2. *Journal of Physical Chemistry C*, 112(17): 6620–6626.

Weavers L K, Malmstadt N, Hoffmann M R, 2000. Kinetics and mechanism of pentachlorophenol degradation by sonication, ozonation, and sonolytic ozonation. *Environmental Science and Technology*, 34(7): 1280–1285.

Xu Z H, Jing C Y, Li F S, Meng X G, 2008. Mechanisms of photocatalytical degradation of monomethylarsonic and dimethylarsinic acids using nanocrystalline titanium dioxide. *Environmental Science and Technology*, 42(7): 2349–2354.

Yang L M, Yu L E, Ray M B, 2009a. Photocatalytic oxidation of paracetamol: dominant reactants, intermediates, and reaction mechanisms. *Environmental Science and Technology*, 43(2): 460–465.

Yang S G, Fu H B, Sun C, Gao Z Q, 2009b. Rapid photocatalytic destruction of pentachlorophenol in F–Si-comodified TiO_2 suspensions under microwave irradiation. *Journal of Hazardous Materials*, 161(2-3): 1281–1287.

Yao W F, Wang H, Xu X H, Zhou J T, Yang X N, Zhang Y et al., 2004. Photocatalytic property of bismuth titanate $Bi_2Ti_2O_7$. *Applied Catalysis A: General*, 259(1): 29–33.

Yin L F, Niu J F, Shen Z Y, Chen J, 2010a. Mechanism of

reductive decomposition of pentachlorophenol by Ti-doped β-Bi_2O_3 under visible light irradiation. *Environmental Science and Technology*, 44(14): 5581–5586.

Yin L F, Shen Z Y, Niu J F, Chen J, Duan Y P, 2010b. Degradation of pentachlorophenol and 2, 4-dichlorophenol by sequential visible-light driven photocatalysis and laccase catalysis. *Environmental Science and Technology*, 44(23): 9117–9122.

Yoon S H, Lee J H, 2005. Oxidation mechanism of As(III) in the UV/TiO_2 system: Evidence for a direct hole oxidation mechanism. *Environmental Science and Technology*, 39(24): 9695–9701.

Yu J C, Ho W, Yu J, Yip H, Wong P K, Zhao J C, 2005. Efficient visible-light-induced photocatalytic disinfection on sulfur-doped nanocrystalline titania. *Environmental Science and Technology*, 39(4): 1175–1179.

Zhang Q Z, Qu X H, Wang H, Xu F, Shi X Y, Wang W X, 2009. Mechanism and thermal rate constants for the complete series reactions of chlorophenols with H. *Environmental Science and Technology*, 43(11): 4105–4112.